

CDKT-FL: Cross-Device Knowledge Transfer using Proxy Dataset in Federated Learning

Minh N. H. Nguyen, Huy Q. Le, Shashi Raj Pandey, and Choong Seon Hong*

Department of Computer Science and Engineering,
Kyung Hee University, Yongin-si 17104, South Korea
{minhnhn, quanghuy69, shashiraj, cshong}@khu.ac.kr

Abstract

In a practical setting towards better generalization abilities of client models for realizing robust personalized Federated Learning (FL) systems, efficient model aggregation methods have been considered as a critical research objective. It is a challenging issue due to the consequences of non-i.i.d. properties of client's data, often referred to as statistical heterogeneity and small local data samples from the various data distributions. Therefore, to develop robust generalized global and personalized models, conventional FL methods need redesigning the knowledge aggregation from biased local models while considering huge divergence of learning parameters due to skewed client data. In this work, we demonstrate that the knowledge transfer mechanism is a de facto technique to achieve these objectives and develop a novel knowledge distillation-based approach to study the extent of knowledge transfer between the global model and local models. Henceforth, our method considers the suitability of transferring the outcome distribution and (or) the embedding vector of representation from trained models during cross-device knowledge transfer using a small proxy dataset in heterogeneous FL. In doing so, we alternatively perform cross-device knowledge transfer following general formulations as 1) global knowledge transfer and 2) on-device knowledge transfer. Through simulations on four federated datasets, we show the proposed method achieves significant speedups and high personalized performance of local models. Furthermore, the proposed approach offers a more stable algorithm than FedAvg during the training, with minimal communication data load when exchanging the trained model's outcomes and representation.

1 Introduction

Nowadays, myriad mobile applications incorporate on-device AI modules to utilize the user's data and facilitate new ex-

*M. N. H. Nguyen, H. Q. Le, S. R. Pandey, and C. S. Hong are with the Department of Computer Science and Engineering, Kyung Hee University, Yongin-si 17104, South Korea.

periences on their smartphones, such as AI-powered cameras, Extended Reality (XR) applications, and intelligent assistants [Samsung, 2021]. However, data privacy concerns have been an *Achille's heels* in the centralized machine learning (ML) paradigm. Thus, in recent years, there's been a sudden surge in developing federated learning (FL) frameworks that's able to limit data privacy leakage [Kairouz *et al.*, 2019; McMahan *et al.*, 2017; Lim *et al.*, 2020]. In FL, a set of devices are connected with a central node (edge/cloud server) to collaboratively train a learning model without sharing their local data [Kairouz *et al.*, 2019]. In doing so, the FL schemes require to share only the learning model parameters to the server; hence, the user data privacy can be kept intact. However, such a federated training scheme raises concerns about the heterogeneity of computing devices and distributed data samples' properties leading to poor learning performance and fluctuation of the trained models across devices. To fill this research gap, recent FL algorithm designs are departing from heterogeneous FL settings towards personalized FL, which considers the performance of the global model and the personalized client models. In *heterogeneous* FL, the underlying data distribution is not identical across devices, i.e., non-i.i.d. Hence, the solution to the global empirical risk minimization problem, i.e., the trained global model, will not *personalize* well for each client. Meanwhile, the local training process in FL algorithms with their small private datasets often results in biased client models that produce high accuracy on the local data but with low generalization capabilities. Also, the client model parameters and data features are diverse across devices. Such as in FedAvg [McMahan *et al.*, 2017], the aggregation of model parameters based on the conventional coordinates-based averaging scheme from highly skewed data could slow down the learning process due to extensive divergence of model parameters to be averaged [Yu *et al.*, 2020].

In this paper, we redesign knowledge transfer mechanisms in FL and examine the underlying fundamental correlation between learning performances of FL algorithms. To that end, we show the proposed method achieves significant speedups and obtains better personalized performance of local models in the fixed users scenario and the subset of users selection scenario. Furthermore, we show our approach offers better stability than the FedAvg algorithm and tackles privacy leakage issues with minimal communication data load when exchanging the trained model's outcomes and (or) representation solely.

In the following subsection, we first outline related approaches to handle the heterogeneity issues in FL literature.

Structural alignment in heterogeneous FL: One of the promising research directions to resolve unmatched parameters of learning models in FL is using the structural alignment methods [Mostafa, 2019; Wang *et al.*, 2020; Yu *et al.*, 2020]. The representation matching in [Mostafa, 2019] and “permutation invariance” in FedMA [Wang *et al.*, 2020] are proposed to evaluate parameter similarity across local models and reorganize the permutation accordingly via matching schemes; thus, obtaining parameters that could be averaged together in the model aggregation. In [Yu *et al.*, 2020], the authors proposed structure-information alignment based on the feature-oriented interpretation and regulation method to ensure explicit feature information allocation in different neural network structures. Based on the feature interpretation, the proposed regulation method adjusts the local model architecture according to their data and task distribution at the very early training stage and continuously maintains structure and information alignment. In this manner, structural alignment methods showed their efficiency in improving the FL performance and applicability in various heterogeneous settings.

Common Representation Learning: This is a popular method to handle the uneven distributions and representations of different modalities or tasks [Bengio *et al.*, 2013; Huang *et al.*, 2017; Peng and Qi, 2019; Xu *et al.*, 2020]. In this approach, the training of shared features across tasks/modalities constructs a common representation; thereby, cross-modal common representational learning allows knowledge transfer across different modalities [Bengio *et al.*, 2013]. In doing so, the heterogeneous data from different modalities resulting in diverse representations are projected into a common space. Then, the cross-modal knowledge transfer can be performed by reducing the discrepancy between representations of pairwise cross-modal data from high-level layers [Huang *et al.*, 2017]. Furthermore, it can preserve the relevant semantics and allow heterogeneous data from different modalities to be correlated more easily [Peng and Qi, 2019; Xu *et al.*, 2020]. Recently, a similar design, the FedRep algorithm [Collins *et al.*, 2021], was applied in FL that alternatively trains the shared low-dimensional representation, which is aggregated across clients by averaging and private local heads to improve the learning performance of client models.

The convergence of the alignment methods and knowledge distillation: Even though the alignment approaches are widely studied in the representation learning literature, the knowledge distillation (KD) approach has emerged as one of the promising alignment approaches. KD approach demonstrated superior performance via knowledge transfer using outcome distribution (i.e., soft targets) from the teacher to student models [Hinton *et al.*, 2015]. The alignment of outcome distribution using Kullback–Leibler (KL) divergence helps the student model imitate and learn from a teacher model or ensemble of models. KD was first introduced in [Bucilua *et al.*, 2006; Ba and Caruana, 2014] and then developed by [Hinton *et al.*, 2015] to compress the smaller learning model from a large model. In KD, the soft targets z_t and z_s are the softmax outputs of the student and teacher model, respectively. The loss function of the student model between the prediction z_s and

ground-truth label y_s is the cross-entropy loss denoted as ℓ_{CE} . In addition, the distillation loss using the KL divergence is defined as

$$\ell_{KD} = \tau^2 KL(z_t, z_s), \quad (1)$$

where τ is the temperature parameter used for softening the output values. The higher the value of the temperature, the softer the outputs of learning models. Therefore, the loss function is used to train the student model is defined as

$$\ell_{\text{student}} = \ell_{CE} + \alpha \ell_{KD}, \quad (2)$$

where α is the hyper-parameter that control the penalty KD loss.

In [Zhang *et al.*, 2018], the authors introduced a deep mutual learning strategy with an ensemble of student models to collaboratively learn and teach each other throughout the training process. Furthermore, KD was recently adopted to transfer the knowledge between the global and local models and exhibited promising results in FL. The alignment of outcome distribution with KL divergence in KD helps the global model and local models to transfer their learning knowledge and further improve the performance of the learning models. To overcome communication cost and heterogeneity issues, the authors in [Jeong *et al.*, 2018] applied KD with the average logits from clients using their private datasets, and balancing the private datasets with data augmentation can further improve the learning performance. The works [Li and Wang, 2019; Bistriz *et al.*, 2020] leveraged a large public dataset in the local knowledge distillation using the aggregation/consensus of soft targets from clients as the teacher knowledge. In [Lin *et al.*, 2020], the authors proposed ensemble distillation for global model fusion enabling different sizes, numerical precision, or structure of learning models. It is possible to apply KD in the global and local model updates, as shown in [He *et al.*, 2020], but the server requires sequentially distilling the knowledge from each client and vice versa. However, the authors do not consider the proxy dataset as well as the knowledge aggregation.

Inspired by the discussion on alignment methods and knowledge distillation approaches, it is fundamental to find the answer to the following research question: “*what transferable knowledge and regularizers should be used in knowledge transfer between the global model and local models in FL?*” Answering this question opens opportunities to provide more efficient knowledge transfer mechanisms in FL.

Contributions: In the typical FL algorithms such as FedAvg [McMahan *et al.*, 2017], FedProx [Li *et al.*, 2020], the global model is updated via model aggregation (i.e., parameters averaging), which is then broadcast back to clients and used as the initial model for local learning. However, such approaches ignore the fundamentals of interleaved properties of data across clients; thus, resulting in poor generalization. To address this research gap, in this work, we propose cross-device knowledge transfer (CDKT) with two mechanisms: 1) global knowledge transfer to transfer the knowledge from client models to the global model, 2) on-device knowledge transfer to transfer the generalized knowledge of the global model to the client models. In doing so, we study the knowledge transfer mechanism using generic distance regularizers

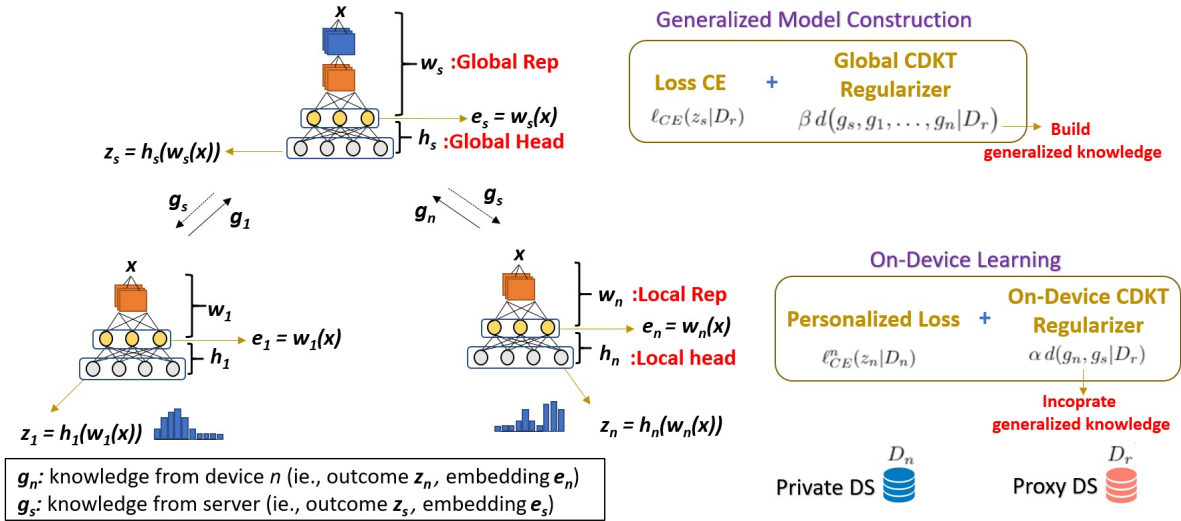


Figure 1: Cross-Device knowledge transfer scheme in FL.

to align the knowledge between the models. Unlike knowledge distillation approaches, the transferable knowledge is the outcomes (i.e., activation results z of the final layer) and (or) embedding representation features (i.e., activation results e of the intermediate layer) given the proxy samples as shown in Fig. 1. We assume this proxy data is of small size and available by clients to follow a practical scenario where the system can pre-collect a small amount of labeled data at the beginning.

Our experiments reveal that (i) the outcome distribution and embedding features’ representation of the proxy data shared by all devices and servers are transferable and (ii) quickly improves the global model performance and personalized performance of the client models. Different from many existing works, we evaluate the personalized performance of local models with specialization (i.e., performance on local testing data), generalization capabilities (i.e., cross-device testing performance). These evaluation metrics provide more insights into the behaviors of the heterogeneous FL systems with different transferring methods and learning settings. The proposed CDKT-FL algorithm enables the flexibility of heterogeneous learning model design and knowledge transfer mechanism for future personalized FL applications. CDKT also improves stability and faster convergence while requiring fewer communication data with outcome and representation knowledge than full complex model parameters compared to the FedAvg algorithm. These observations provide solid motivation to study knowledge transfer approaches and related metrics in FL.

2 Cross-Device Knowledge Transfer in Federated Learning

In a general scheme of FL algorithms [Reddi *et al.*, 2020; Li *et al.*, 2021], the global model is updated via a gradient-based optimizer or model parameter aggregation in the server, while the local/personalized model in user device n is updated using their private dataset D_n . We first define the neural net-

work with the prediction outcomes (i.e., $z = h \circ w(x)$), where h is the projection head, which is a small neural network (i.e., the last fully-connected layers; a small classifier). We denote the embedding features of the representation sub-net parameters w for the image x as $e = w(x)$. Hence, the learning model parameters w, h can be trained and used to extract the embedding features (i.e., e_n) and (or) classes’ prediction distribution (i.e., z_n) of input images at device n . In this work, instead of using model parameters from clients in every round to aggregate into the global model, cross-device knowledge transfer is being used to transfer the collective knowledge from all clients to the server and construct a generalized model. Note that the global model can be updated using an additional regularizer to align its knowledge with the collective knowledge of clients. In doing so, it is necessary to have a fixed small proxy data D_r such that all models can access and provide their learning knowledge as the outcomes (i.e., z) and (or) embedding features (i.e., e), as shown in Fig. 1. In addition, the knowledge transfer also helps the global model transfer its generalization capability to all client models. This way, firstly, we can reduce communication data load and also further enhance users’ data privacy, which is often compromised during full parameters exchange against reverse engineering tricks. Secondly, since the knowledge transfer is sufficient to transfer learning capabilities, the learning model architectures can differ between the server model (with more layers) and client models (with fewer layers). Towards that end, in Fig. 1, we illustrate the proposed scheme of CDKT-FL.

The proposed CDKT-FL algorithm (Alg. 1) enables the transfer of knowledge between clients and global models in the FL setting. At each global round t , the server broadcasts the knowledge from the updated global model to all clients. Then, each client performs K local epochs with its private and proxy dataset based on the gradient of the loss function in the *on-device learning* problem (8), with the local learning rate η . Note that we use mini-batch of private data in the cross-entropy loss, whereas proxy data in the on-device CDKT

regularizer. Then, the clients send their latest knowledge (i.e., z_n and (or) e_n) to the server. At the global level, the server builds the generalized model by solving the global learning problem (5). For this, we use a gradient-based update for R global epochs with the global learning rate γ . In particular, to perform CDKT-FL, we design the knowledge transfer in FL with two general problems: *generalized model construction* and *on-device learning* in the following subsections.

2.1 Generalized Model Construction

In the generalized model construction problem, the main target is utilizing the proxy data (i.e., D_r) and collective knowledge from all devices to build the global model. If the transferable knowledge is only the outcome of client models, then the problem is in the form of knowledge distillation (KD) [Hinton *et al.*, 2015]. Similar to the design of [Li and Wang, 2019], we consider the averaged results of the outcomes as the collective knowledge that results in the equivalent performance of the learning problem. This approach, however, requires less computation than the sum of individual KL loss between the student model (global model) and each teacher model (client model) in ensemble KD. In the following, we review the KD method and discuss the proposed cross-device knowledge transfer method.

- *KD Method:*

$$\ell_s(D_r) = \ell_{CE}(z_s|D_r) + \beta \ell_{KD}\left(z_s, \sum_{n \in N} \frac{1}{N} z_n | D_r\right), \quad (3)$$

where β is the parameter to control the trade-off between proxy data loss and the KD regularizer; z are the soft targets of the learning models.

- *Cross-device knowledge transfer Method (CDKT):* We formulate the general generalized model construction problem with the global CDKT regularizer using a generic function d . Thereby, the proposed formulation measures the discrepancy between the knowledge of n client models (g_1, \dots, g_n) and the knowledge of server model g_s as

$$\ell_s(D_r) = \ell_{CE}(z_s|D_r) + \beta d(g_s, g_1, \dots, g_n | D_r). \quad (4)$$

The collective knowledge from clients are constructed as the averaged results of the outcomes z and (or) embedding features e . To improve the limitation in transferred knowledge from clients, we adjust the collective outcomes z of clients by averaging it with the true labels y_r when using their final outcomes.

$$\begin{aligned} \ell_s(D_r) = & \ell_{CE}(z_s|D_r) + \beta d\left(e_s, \sum_{n \in N} \frac{1}{N} e_n | D_r\right) \\ & + \beta d\left(z_s, \lambda y_r + (1 - \lambda) \sum_{n \in N} \frac{1}{N} z_n | D_r\right), \end{aligned} \quad (5)$$

where $\lambda \in [0, 1]$, and the parameter β allows the server to control the trade-off between proxy data loss and the global CDKT regularizer. Here, we note that various distance functions d can be used for knowledge transfer, such as Norm, KL divergence, and Jensen-Shannon

Algorithm 1 CDKT-FL Algorithm

- 1: **Input:** T, K, R
 - 2: **for** $t = 0, \dots, T - 1$ **do**
 - 3: **On-Device Learning:** Each device n receives the generalized knowledge g_s from the server and updates local model with D_n, D_r ;
 - 4: **for** $k = 0, \dots, K - 1$ **do**
 - 5: We loop for each batch of private and proxy data (i.e., S_n and S_r):

$$w_n^t = w_n^t - \eta \nabla \ell_c^n(S_n, S_r); \quad (6)$$
 - 6: **end for**
 - 7: Device n extracts and sends the local knowledge g_n given the proxy dataset to the server;
 - 8: **Generalized Model Construction:** Server updates the global model with the received local knowledge from the selected devices:
 - 9: **for** $r = 0, \dots, R - 1$ **do**
 - 10: We loop through batches of proxy data (i.e., S_r):

$$w_g^t = w_g^t - \gamma \nabla \ell_s(S_r) \quad (7)$$
 - 11: **end for**
 - 12: **end for**
-

(JS) divergence [Kullback, 1997]. We provide the concrete mathematical formulations of these distances in our supplementary materials.

2.2 On-device Learning

Using a similar design, the on-device learning problem helps the client models to improve their generalization capabilities by imitating the generalized knowledge from the global model. In this approach, the client n utilizes the private dataset D_n and also the generalized knowledge from the global model obtained using the proxy dataset D_r . In particular, we formulate the on-device loss function for each device n as follows:

$$\begin{aligned} \ell_c^n(D_n, D_r) &= \ell_{CE}^n(z_n | D_n) + \alpha d(g_n, g_s | D_r) \\ &= \ell_{CE}^n(z_n | D_n) + \alpha d(e_n, e_s | D_r) \\ &\quad + \alpha d(z_n, \lambda y_s + (1 - \lambda) z_s | D_r) \end{aligned} \quad (8)$$

where α is the parameter to control the trade-off between the local learning objective's biased knowledge and generalization capabilities. Further, the on-device CDKT regularizer helps to reduce the bias and over-fitting issues of local models when training on the small private dataset.

3 Experiments

3.1 Setting

In this section, we validate the efficacy of the CDKT-FL algorithm with the MNIST [LeCun *et al.*, 1998], Fashion-MNIST [Xiao *et al.*, 2017], CIFAR-10, and CIFAR-100 [Krizhevsky *et al.*, 2009] datasets for handwritten digits, fashion images, and objects recognition, respectively. We conduct the experiments with 10 selected clients in each round, where each client has median numbers of data samples at 63, 70.5, 966.5, and

Table 1: The median of testing accuracy on four datasets from 90 to 100 rounds

		Fashion-MNIST		MNIST		CIFAR-10		CIFAR-100	
		Global	C-Per	Global	C-Per	Global	C-Per	Global	C-Per
Fixed Users	No Transfer	83.72	59.09	81.14	59.70	55.92	50.43	17.27	18.76
	FedAvg	82.56	76.41	90.12	87.20	59.85	52.95	15.53	17.13
	CDKT (Rep)	84.88	86.06	86.22	90.09	58.44	59.25	17.75	21.81
	CDKT (Full)	85.81	81.66	88.02	85.70	58.91	55.83	17.84	21.93
	CDKT (RepFull)	86.51	84.08	88.32	87.25	59.09	57.74	18.49	22.22
Subset of Users	No Transfer	78.19	58.98	80.50	58.06	52.17	46.75	16.47	8.13
	FedAvg	69.44	70.62	88.03	89.18	48.83	47.20	12.25	12.57
	CDKT (Rep)	78.50	80.90	84.75	84.61	55.67	53.92	16.72	15.74
	CDKT (Full)	79.22	79.02	85.91	79.32	56.60	54.35	17.33	15.76
	CDKT (RepFull)	79.94	81.39	84.62	81.82	56.57	54.03	17.60	17.74

1163.5 with MNIST, Fashion-MNIST, CIFAR-10, and CIFAR-100 respectively. To simulate the properties of non-i.i.d data distribution, we set each client’s data from random 20 classes in 100 classes for CIFAR-100 dataset and only two classes in total 10 classes with the other datasets, and use 20% of private data samples for evaluating the testing performance. Thereby, the private datasets are unbalanced and have a small number of training samples. Further, the small proxy datasets have all classes data with, respectively, 355, 330, 4200, and 4200 samples for MNIST, Fashion-MNIST, and CIFAR-10 datasets. The global CNN model in the server consists of two convolution layers in MNIST and Fashion-MNIST dataset, whereas three convolution layers are used in the CIFAR-10 and CIFAR-100 dataset, followed by the pooling and fully connected layers. The client CNN models have a similar design or one CNN layer fewer than the global model one in the heterogeneous model setting. The learning parameters such as learning rates, trade-off parameters are tuned to achieve good results for different settings of algorithms; the number of local epochs $K = 2$, global epochs $R = 2$, and the batch size is 20.

Evaluation metrics: To the best of our knowledge, FL approaches focus more on the learning performance of the global model while personalized FL algorithms evaluate the learning performance of the local models. In this work, to better capture the learning behavior of FL algorithms, we conduct evaluations with the specialization (**C-Spec**) and generalization (**C-Gen**) performance of client models on average, defined by the accuracy in their local testing data only, and the collective testing data from all clients, respectively. To summarize the performance of local models, we calculate the average of **C-Gen** and **C-Spec** performance as the **C-Per** metric. Meanwhile, the **Global** metric is the accuracy of the global model for the collective testing data from all clients.

Baselines and CDKT settings: For comparison, we evaluate different settings of the CDKT-FL algorithm and compared them with the FedAvg algorithm, no transfer knowledge scheme. Accordingly, the setting **Rep**, **Full**, and **RepFull** stand for using only the embedding features of representation, outcomes of full models, and both in the global knowledge transfer, respectively. Furthermore, different distance functions were also validated, such as KL, JS, and Norm-2 (N). The setting KL-N indicates the use of KL divergence in the global

CDKT regularizer, while the on-device CDKT regularizer uses Norm-2.

3.2 Experimental Results

In summary, we obtained experimental results on four datasets for different settings in the CDKT-FL algorithm and baselines with the median testing accuracy from round 90 to 100, as in Table 1. There are two principal scenarios: (1) fixed 10 users, and (2) selected 10 from the total 50 users. Compared to the FedAvg algorithm, CDKT-FL outperforms 10% with Fashion-MNIST, 7% with CIFAR-10, 5% for both scenarios according to **C-Per** performance. Meanwhile in MNIST, CDKT-FL obtains 3% better in scenario (1) but 4% lower **C-Per** performance than FedAvg in scenario (2). In addition to the main target to improve personalized performance, CDKT-FL also significantly improves the performance of global model in most of the settings except MNIST dataset. According our detailed figures, in scenario (1), CDKT-FL obtains higher **C-Gen** performance, a comparable **C-Spec** performance of client models, and a comparable or higher **Global** performance. In scenario (2), our proposed algorithm achieves higher **C-Spec** and **Global** performance with the Fashion-MNIST and CIFAR datasets, but FedAvg exceptionally exhibits a good performance on a simple learning task such as hand digit recognition on MNIST dataset. In principle, CDKT helps the client models improve **C-Gen** and slightly improve the **Global** performance than that of no transfer setting. The detailed results for MNIST and CIFAR-10 datasets are shown in our supplementary material. In addition, as the final performance metric, CDKT-FL algorithm exhibits better stability and faster convergence in general while improving the **C-Per**, and preserves high **Global** performance in most of the settings. These attributes also enable the client or global models to be usable early after 50 communication rounds. As expected, in the subset of users selection scenario, the FedAvg algorithm shows an extensive fluctuation due to irregularity in learning parameters across the client models stemmed from statistical heterogeneity.

In Fig. 2, we evaluate different settings knowledge transfer schemes of CDKT-FL to compare with No transfer and FedAvg in both of the scenarios on Fashion-MNIST dataset. In scenario (1), as shown in Fig. 2a, experimental results demonstrate that our proposed schemes outperform the baselines in terms of speedups **C-Gen** and **Global** performance. The

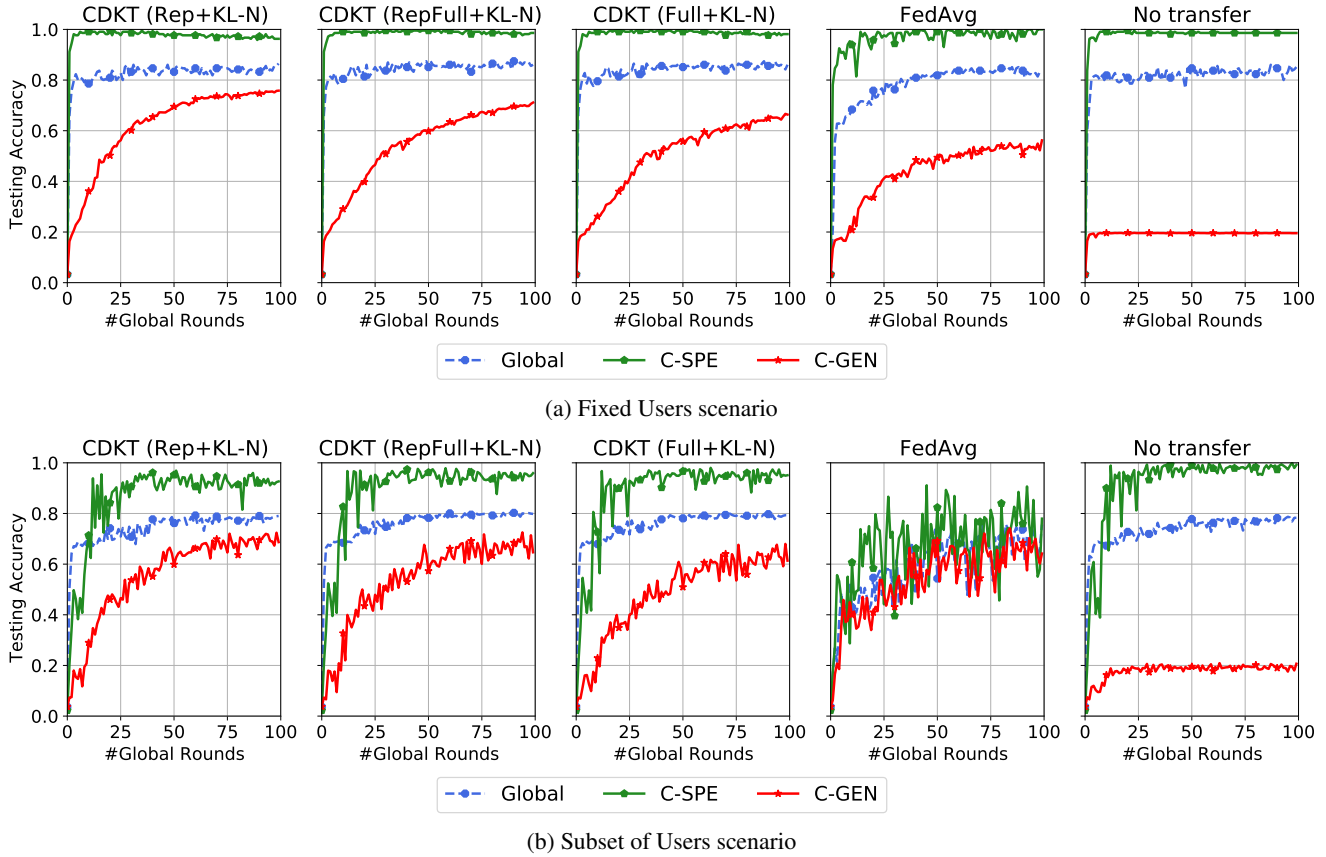


Figure 2: Comparison of CDKT-FL with different settings versus FedAvg and No Transfer with Fashion-MNIST dataset

Rep+KL-N setting achieves the highest **C-Gen** performance with 75.37% but slightly lower **C-Spec** than that of FedAvg. In scenario (2), Fig. 2b shows that the CDKT-FL algorithms with three settings significantly improve **C-Spec**, **Global** and more stable than FedAvg algorithm.

In the supplemental material, we evaluate the effects of the trade-off parameters used to control the compensation between learning loss and the CDKT regularizer. As a result, when increasing α , we can boost **C-Gen** performance; however, that slightly degrades the **C-Spec** performance. Such learning behavior shows the interesting compensation effect between **C-Gen** and **C-Spec** performances, such as till some threshold the specialized capability may decrease as increasing the generalized capability of client models. On the other hand, β does not show significant effects on the performance, however, when β is too small, it makes the global performance is fluctuated due to less contribution from CDKT regularizers and transferred knowledge. Finally, we evaluate the effectiveness of the CDKT-FL algorithm using heterogeneous local models, i.e., using one CNN layer less than global model. The CDKT-FL algorithm with smaller client models achieves comparable performance in Fashion-MNIST dataset but slight degradation in the other datasets.

4 Conclusion

This work bridges the gap between existing alignment methods and knowledge distillation to develop a general form of cross-device knowledge transfer in FL. Numerous experiments, settings, regularizers, and scenarios are validated to study the performance of client and global models for a better understanding of their behaviors in heterogeneous FL. The detailed results following extensive simulations on four datasets have shown the advantages of the proposed algorithms. Compared to the FedAvg algorithm, we demonstrate that the CDKT-FL algorithm is more stable and can speed up the global model performance, higher personalized performance of client models. In addition to the learning performance, the proposed algorithm enables (i) the flexibility of heterogeneous model architectures, (ii) reduces communication data with the outcome and (or) representation knowledge instead of full model parameters compared to the conventional FL algorithms, and (iii) tackles privacy leakage issues (via reverse engineering techniques) of current FL algorithms. Finally, we advocate the knowledge transfer method works as a hybrid design with recent advanced techniques to improve learning performance.

References

[Ba and Caruana, 2014] Jimmy Ba and Rich Caruana. Do deep nets really need to be deep? In *Advances in Neural*

- Information Processing Systems*, volume 27, 2014.
- [Bengio *et al.*, 2013] Yoshua Bengio, Aaron Courville, and Pascal Vincent. Representation learning: A review and new perspectives. *IEEE Transactions on Pattern Analysis and Machine Intelligence*, 35(8):1798–1828, 2013.
- [Bistriz *et al.*, 2020] Ilai Bistriz, Ariana Mann, and Nicholas Bambos. Distributed distillation for on-device learning. In *Advances in Neural Information Processing Systems*, volume 33, pages 22593–22604, 2020.
- [Buciluă *et al.*, 2006] Cristian Buciluă, Rich Caruana, and Alexandru Niculescu-Mizil. Model compression. In *Proceedings of the 12th ACM SIGKDD international conference on Knowledge discovery and data mining*, pages 535–541, 2006.
- [Collins *et al.*, 2021] Liam Collins, Hamed Hassani, Aryan Mokhtari, and Sanjay Shakkottai. Exploiting shared representations for personalized federated learning. In *Proceedings of the 38th International Conference on Machine Learning*, volume 139, pages 2089–2099, 18–24 Jul 2021.
- [He *et al.*, 2020] Chaoyang He, Murali Annavaram, and Salman Avestimehr. Group knowledge transfer: Federated learning of large cnns at the edge. In *Advances in Neural Information Processing Systems*, volume 33, 2020.
- [Hinton *et al.*, 2015] Geoffrey Hinton, Oriol Vinyals, and Jeffrey Dean. Distilling the knowledge in a neural network. In *NIPS Deep Learning and Representation Learning Workshop*, 2015.
- [Huang *et al.*, 2017] Xin Huang, Yuxin Peng, and Mingkuan Yuan. Cross-modal common representation learning by hybrid transfer network. In *Proceedings of the 26th International Joint Conference on Artificial Intelligence*, pages 1893–1900, 2017.
- [Jeong *et al.*, 2018] Eunjeong Jeong, Seungeun Oh, Hyesung Kim, Jihong Park, Mehdi Bennis, and Seong-Lyun Kim. Communication-efficient on-device machine learning: Federated distillation and augmentation under non-iid private data. *arXiv:1811.11479*, 2018.
- [Kairouz *et al.*, 2019] Peter Kairouz, H Brendan McMahan, Brendan Avent, Aurélien Bellet, Mehdi Bennis, Arjun Nitin BhagCanhoji, Keith Bonawitz, Zachary Charles, Graham Cormode, Rachel Cummings, et al. Advances and open problems in federated learning. *arXiv:1912.04977*, 2019.
- [Krizhevsky *et al.*, 2009] Alex Krizhevsky, Geoffrey Hinton, et al. Learning multiple layers of features from tiny images. 2009.
- [Kullback, 1997] Solomon Kullback. *Information theory and statistics*. Courier Corporation, 1997.
- [LeCun *et al.*, 1998] Yann LeCun, Léon Bottou, Yoshua Bengio, and Patrick Haffner. Gradient-based learning applied to document recognition. *Proceedings of the IEEE*, 86(11):2278–2324, 1998.
- [Li and Wang, 2019] Daliang Li and Junpu Wang. Fedmd: Heterogenous federated learning via model distillation. In *The 2nd International Workshop on Federated Learning for User Privacy and Data Confidentiality*, 2019.
- [Li *et al.*, 2020] Tian Li, Anit Kumar Sahu, Manzil Zaheer, Maziar Sanjabi, Ameet Talwalkar, and Virginia Smith. Federated optimization in heterogeneous networks. In *Proceedings of Machine Learning and Systems 2020*, pages 429–450. 2020.
- [Li *et al.*, 2021] Tian Li, Shengyuan Hu, Ahmad Beirami, and Virginia Smith. Ditto: Fair and robust federated learning through personalization. In *International Conference on Machine Learning*, pages 6357–6368. PMLR, 2021.
- [Lim *et al.*, 2020] Wei Yang Bryan Lim, Nguyen Cong Luong, Dinh Thai Hoang, Yutao Jiao, Ying-Chang Liang, Qiang Yang, Dusit Niyato, and Chunyan Miao. Federated learning in mobile edge networks: A comprehensive survey. *IEEE Communications Surveys & Tutorials*, 22(3):2031–2063, 2020.
- [Lin *et al.*, 2020] Tao Lin, Lingjing Kong, Sebastian U Stich, and Martin Jaggi. Ensemble distillation for robust model fusion in federated learning. In *Advances in Neural Information Processing Systems*, volume 33, pages 2351–2363, 2020.
- [McMahan *et al.*, 2017] Brendan McMahan, Eider Moore, Daniel Ramage, Seth Hampson, and Blaise Aguera y Arcas. Communication-efficient learning of deep networks from decentralized data. In *Artificial Intelligence and Statistics*, pages 1273–1282, 2017.
- [Mostafa, 2019] Hesham Mostafa. Robust federated learning through representation matching and adaptive hyperparameters. *arXiv:1912.13075*, 2019.
- [Peng and Qi, 2019] Yuxin Peng and Jinwei Qi. Cm-gans: Cross-modal generative adversarial networks for common representation learning. *ACM Transactions on Multimedia Computing, Communications, and Applications (TOMM)*, 15(1):1–24, 2019.
- [Reddi *et al.*, 2020] Sashank J Reddi, Zachary Charles, Manzil Zaheer, Zachary Garrett, Keith Rush, Jakub Konečný, Sanjiv Kumar, and Hugh Brendan McMahan. Adaptive federated optimization. In *International Conference on Learning Representations*, 2020.
- [Samsung, 2021] Samsung. Smarter future powered by ai. [samsung.com/semiconductor/minisite/exynos/technology/ai/](https://www.samsung.com/semiconductor/minisite/exynos/technology/ai/), 2021.
- [Wang *et al.*, 2020] Hongyi Wang, Mikhail Yurochkin, Yuekai Sun, Dimitris Papailiopoulos, and Yasaman Khazaeni. Federated learning with matched averaging. In *International Conference on Learning Representations*, 2020.
- [Xiao *et al.*, 2017] Han Xiao, Kashif Rasul, and Roland Vollgraf. Fashion-mnist: a novel image dataset for benchmarking machine learning algorithms. *arXiv:1708.07747*, 2017.
- [Xu *et al.*, 2020] Xing Xu, Kaiyi Lin, Lianli Gao, Huimin Lu, Heng Tao Shen, and Xuelong Li. Learning cross-modal common representations by private-shared subspaces separation. *IEEE Transactions on Cybernetics*, 2020.

[Yu *et al.*, 2020] Fuxun Yu, Weishan Zhang, Zhuwei Qin, Zirui Xu, Di Wang, Chenchen Liu, Zhi Tian, and Xiang Chen. Heterogeneous federated learning. *arXiv:2008.06767*, 2020.

[Zhang *et al.*, 2018] Ying Zhang, Tao Xiang, Timothy M Hospedales, and Huchuan Lu. Deep mutual learning. In *Proceedings of the IEEE Conference on Computer Vision and Pattern Recognition*, pages 4320–4328, 2018.

5 Supplemental Results

In this material, we added Table 1, 2 for the detailed **C-Gen** and **C-Spec** of algorithms with four datasets. For each dataset, we also use the box plots to illustrate the fluctuation of algorithm from 90 to 100 rounds. As can be seen, our algorithm obtains a stable convergence with better performance while FedAvg depicts the extensive fluctuation, especially in the subset of users scenario.

5.1 Cross Entropy Loss:

$$\ell_{CE}(z|D_r) = - \sum_{x \in D_r} \sum_c P(y_c|x) \ln P(z_c|x),$$

where $P(z_c|x)$ is the prediction outcome probability and $P(y_c|x)$ is the target label of class c given data sample x .

5.2 Distance for the CDKT regularizers:

A generic distance function d in CDKT regularizer can be adopted with three following distance metrics

- Norm2 distance:

$$d_{norm}(g_n, g_s|D_r) = \sum_{x \in D_r} \|g_n(x) - g_s(x)\|_2,$$

where $g_n(x)$ is the prediction outcome (or embedding features) of client n and $g_s(x)$ is the knowledge from global model given data sample x .

- Kullback–Leibler (KL) divergence:

$$d_{KL}(g_n, g_s|D_r) = \sum_{x \in D_r} \sum_c P(g_{s,c}|x) \frac{P(g_{n,c}|x)}{P(g_{s,c}|x)},$$

where $P(g_{n,c}|x)$ is the prediction outcome (or embedding features) of client n and $P(g_{s,c}|x)$ is the knowledge from global model of class c given data sample x .

- Jashon-Shannon (JS) divergence:

$$d_{JS}(g_n, g_s|D_r) = \frac{1}{2}d_{KL}(g_n, g_m|D_r) + \frac{1}{2}d_{KL}(g_s, g_m|D_r)$$

where $g_m = \frac{1}{2}(g_n + g_s)$.

5.3 Additional Fashion-MNIST results

For Fashion-MNIST, we evaluate the effect of trade-off parameters α and β as shown in Fig. 4, 5. We also evaluate the effect of different distance metrics in CDKT-regularizers in both scenarios in Fig. 6. We observe that the setting KL-N obtains stable and higher performance among other metrics. In the KL-N setting, KL divergence is used in the global CDKT regularizer, while the on-device CDKT regularizer uses Norm.

5.4 MNIST results

Similar to Fashion-MNIST, we also provide the detailed figures in this subsection. In Fig. 8, we evaluate the different transferred knowledge with CDKT-FL algorithm and compare with FedAvg and No transfer in both scenarios. In scenario (1), our algorithm depicts the fast convergence on **C-Gen** performance after just 30 rounds while FedAvg requires nearly 80 rounds to reach stability and comparable performance. Regarding the subset of users scenario, our algorithm obtains the better **C-Spec**, global performance and lower **C-Gen** performance than FedAvg. Nevertheless, FedAvg experiences an extensive fluctuation despite the high **C-Gen** performance. Similar to the Fashion-MNIST, the results indicate that the setting KL-N achieves the best performance among others metrics in both scenarios as shown in Fig. 9. Finally, we observe that our method obtains the comparable performance when using heterogeneous models in Fig. 10 with just a slight degradation in fixed users scenario.

5.5 CIFAR-10 and CIFAR-100 results

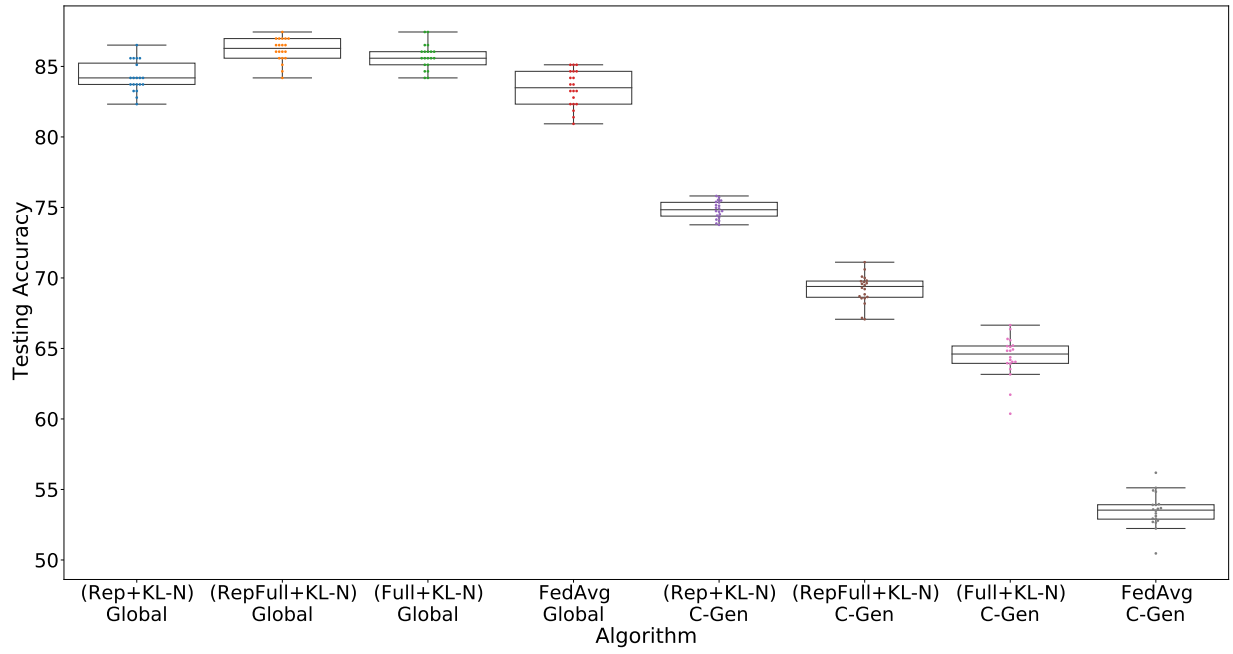
Similar to the learning behaviors with the Fashion-MNIST dataset in the main manuscript, CIFAR-10 and CIFAR-100 exhibit faster convergence of the **Global** and **C-Gen** performance and its stability with different transferred knowledge as shown in Fig. 12 and Fig. 15, respectively, in scenario (1). Regarding scenario (2), FedAvg depicts the slightly higher **C-Gen** performance, meanwhile CDKT-FL outperforms FedAvg in terms of **Global** and **C-Spec** performance. CDKT-FL shows a slight degradation in the last 20 global rounds with the highest **C-Gen** performance. Also, FedAvg extensively fluctuates since the learned models are highly different between clients. Moreover, as shown in Fig. 13 and Fig. 16, using smaller learning models at clients with two CNN layers while three CNN layers in the server model shows a slight degradation due to lower learning capacities in both datasets.

Table 2: The median of testing accuracy on four datasets from 90 to 100 rounds in fixed users scenario

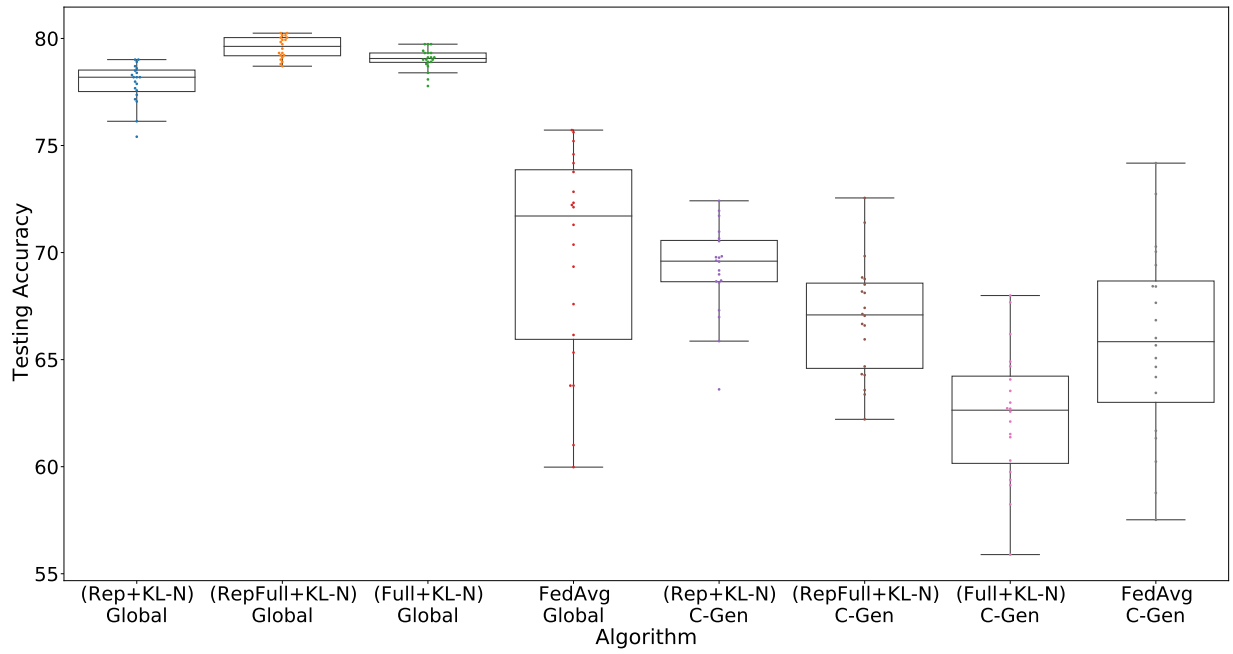
	Fashion-MNIST			MNIST			CIFAR-10			CIFAR-100		
	<i>Global</i>	<i>C-Gen</i>	<i>C-Spe</i>	<i>Global</i>	<i>C-Gen</i>	<i>C-Spe</i>	<i>Global</i>	<i>C-Gen</i>	<i>C-Spe</i>	<i>Global</i>	<i>C-Gen</i>	<i>C-Spe</i>
No Transfer	83.72	19.58	98.60	81.14	21.80	97.60	55.92	22.74	78.11	17.27	8.29	29.23
FedAvg	82.56	53.05	98.14	90.12	76.30	98.20	59.85	26.24	79.66	15.53	7.58	26.67
CDKT (Rep)	84.88	75.37	96.74	86.22	81.98	98.20	58.44	40.59	77.91	17.75	12.27	31.34
CDKT (Full)	85.81	65.19	98.14	88.02	73.20	98.20	58.91	37.93	73.74	17.84	11.06	32.80
CDKT (RepFull)	86.51	69.70	98.37	88.32	76.29	98.20	59.09	39.88	75.59	18.49	11.69	32.76

Table 3: The median of testing accuracy on four datasets from 90 to 100 rounds in subset of users scenario

	Fashion-MNIST			MNIST			CIFAR-10			CIFAR-100		
	<i>Global</i>	<i>C-Gen</i>	<i>C-Spe</i>	<i>Global</i>	<i>C-Gen</i>	<i>C-Spe</i>	<i>Global</i>	<i>C-Gen</i>	<i>C-Spe</i>	<i>Global</i>	<i>C-Gen</i>	<i>C-Spe</i>
No Transfer	78.19	19.09	98.86	80.50	18.68	97.45	52.17	17.14	76.35	16.47	3.04	13.22
FedAvg	69.44	65.33	75.90	88.03	86.06	92.30	48.83	41.69	52.70	12.25	10.81	14.34
CDKT (Rep)	78.50	69.70	92.10	84.75	72.38	96.85	55.67	38.33	69.52	16.72	7.41	24.07
CDKT (Full)	79.22	62.86	95.17	85.91	62.81	95.83	56.60	38.02	70.69	17.33	7.76	23.76
CDKT (RepFull)	79.94	67.82	94.96	84.62	66.84	96.81	56.57	38.85	69.22	17.60	10.32	25.15



(a) Fixed Users Scenario



(b) Subset of Users Scenario

Figure 3: Convergence of CDKT-FL with different settings versus FedAvg with Fashion-MNIST dataset

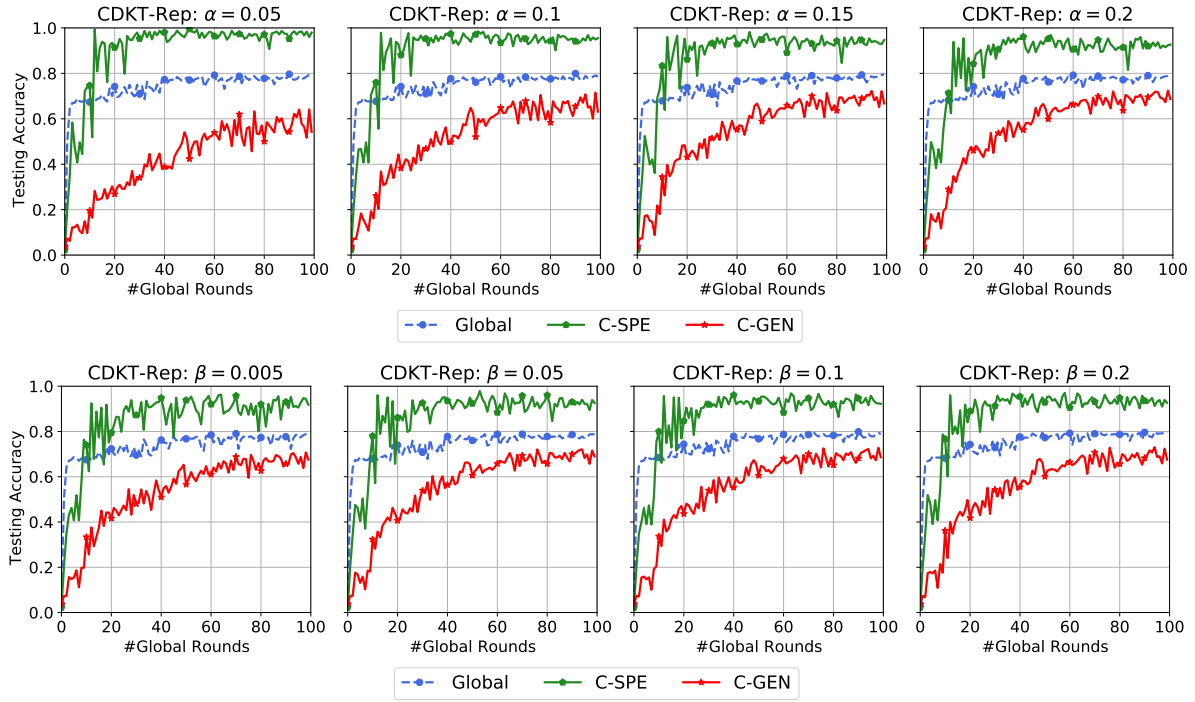


Figure 4: Effects of trade-off parameters in CDKT-FL with Fashion-MNIST dataset

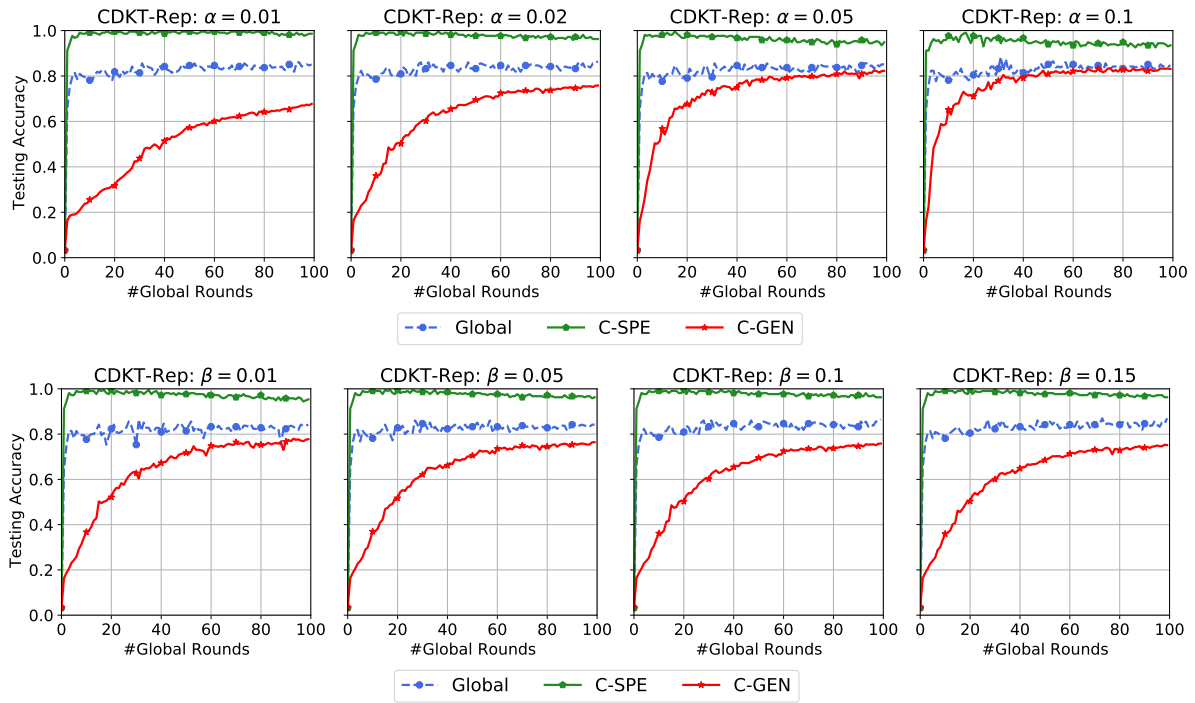
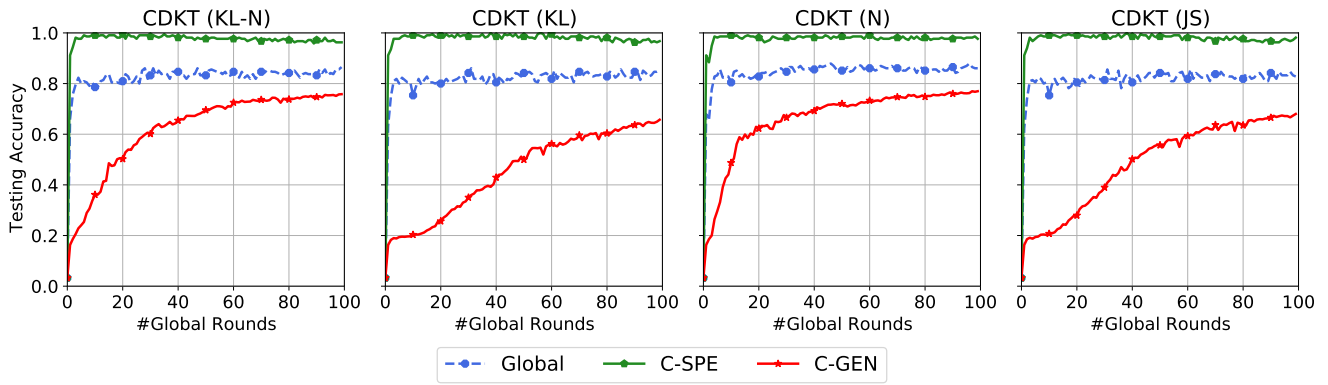
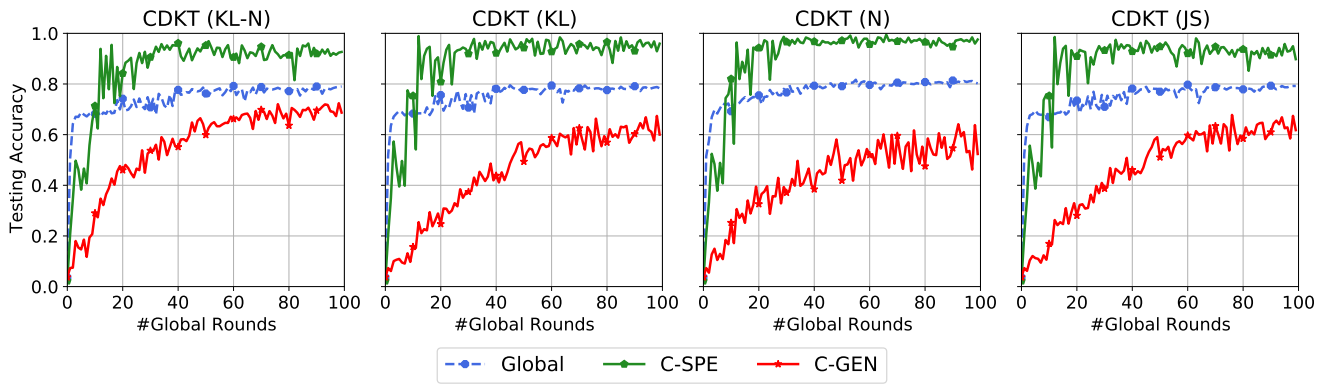


Figure 5: Effects of trade-off parameters in CDKT-FL with Fashion-MNIST dataset



(a) Fixed Users Scenario



(b) Subset of Users Scenario

Figure 6: Distance metric comparison of CDKT-FL with Fashion-MNIST dataset

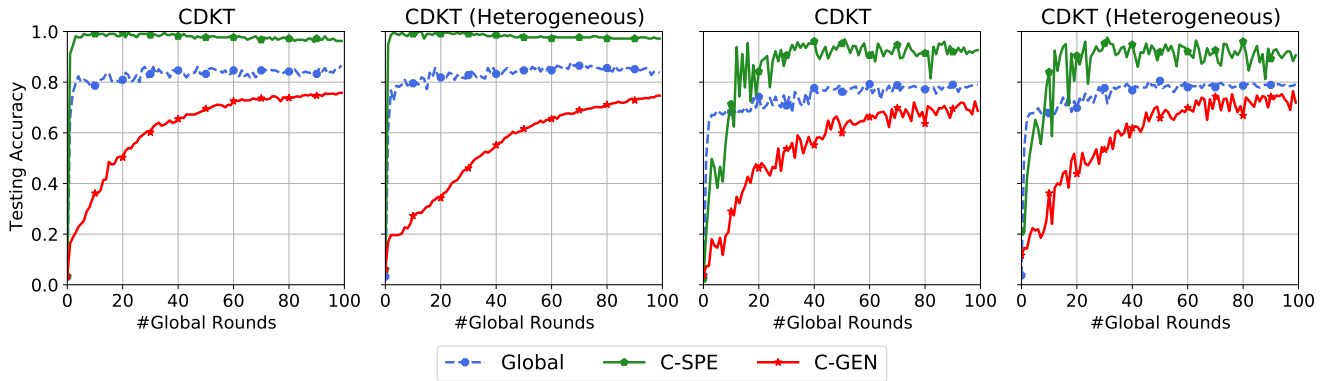
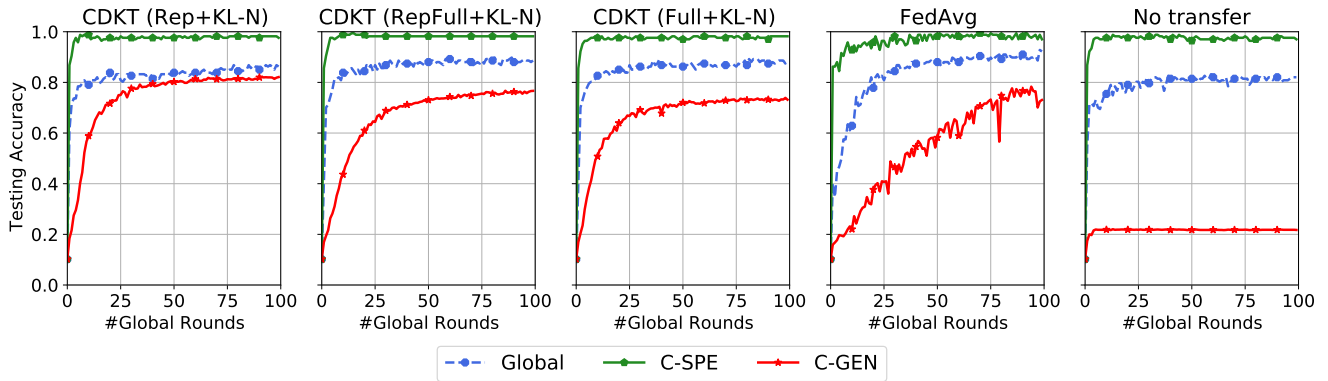
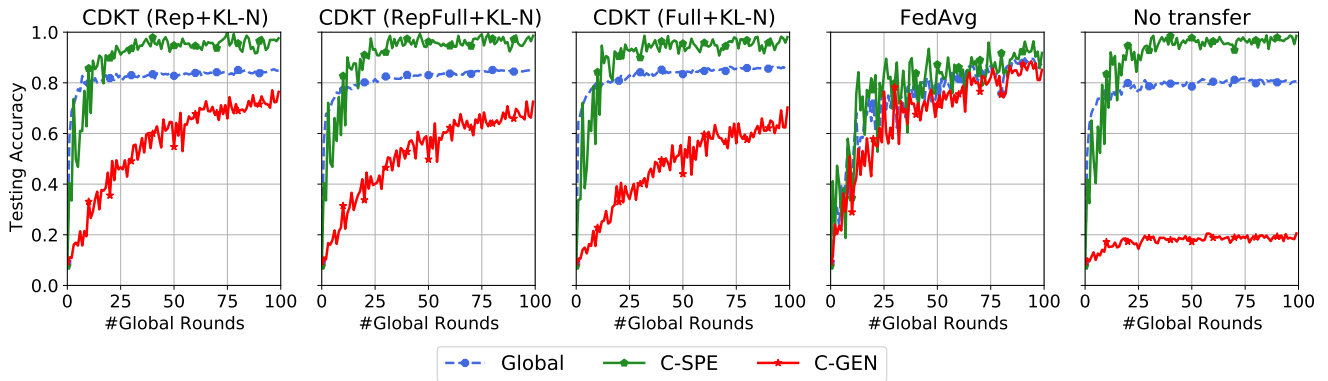


Figure 7: Comparison between Homogeneous and Heterogeneous model with Fashion-MNIST dataset

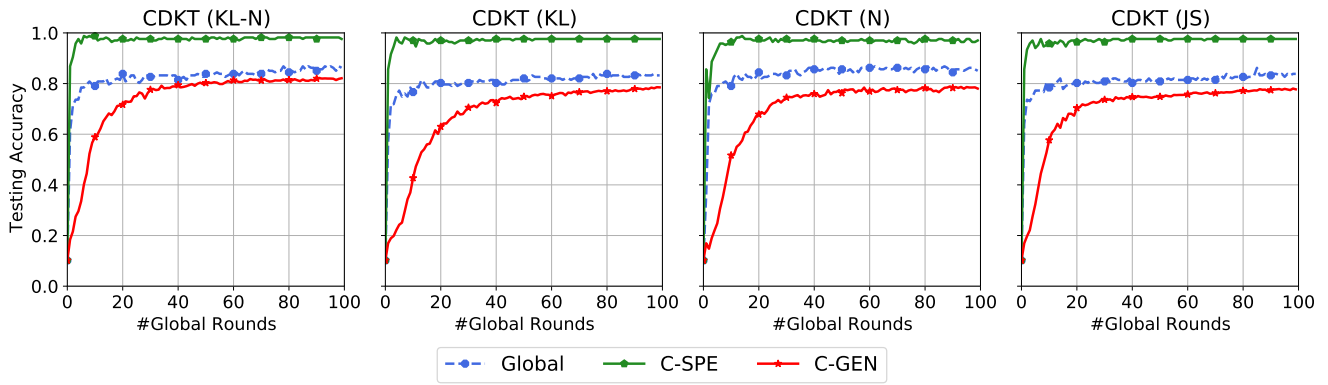


(a) Fixed Users Scenario

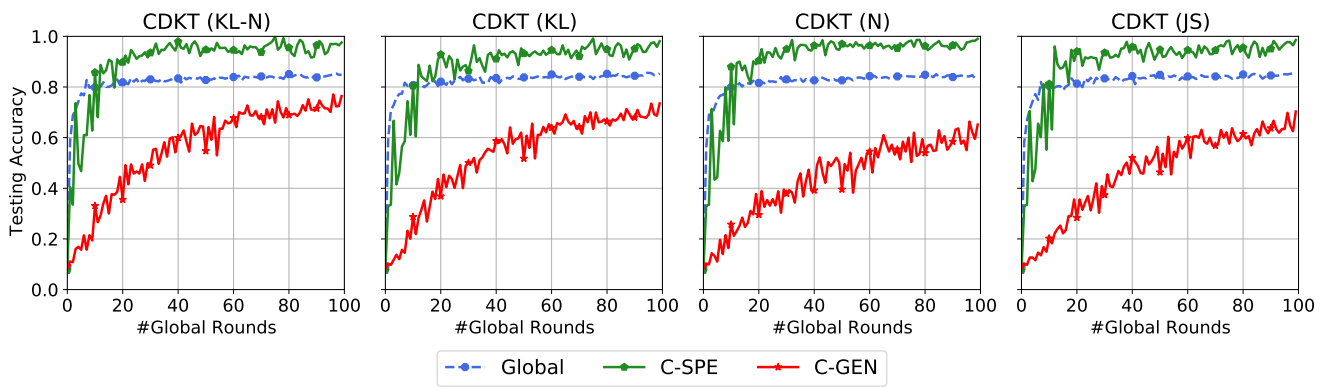


(b) Subset of Users Scenario

Figure 8: Comparison of CDKT-FL with different settings versus FedAvg and No Transfer with MNIST dataset



(a) Fixed Users Scenario



(b) Subset of Users Scenario

Figure 9: Distance metric comparison of CDKT-FL with MNIST dataset

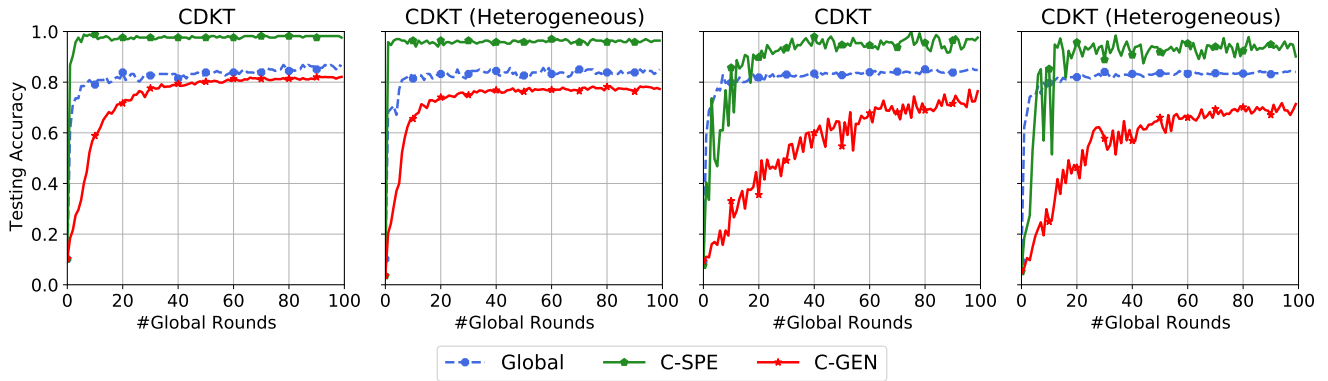
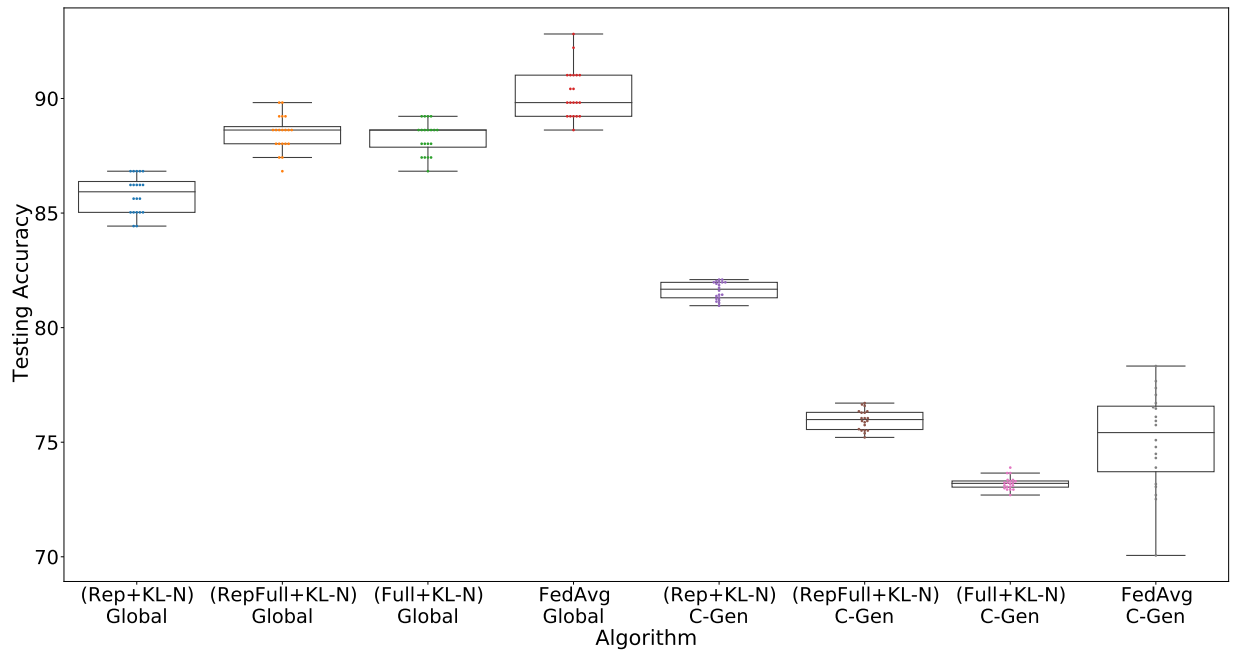
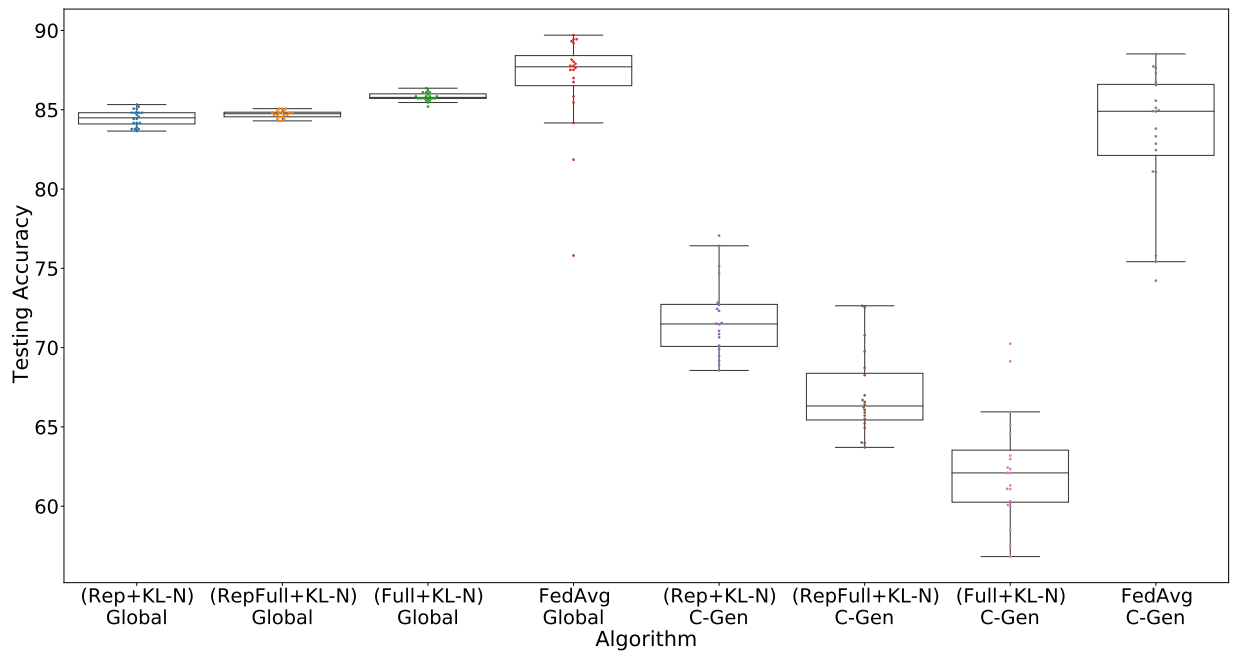


Figure 10: Comparison between Homogeneous and Heterogeneous Model with MNIST dataset

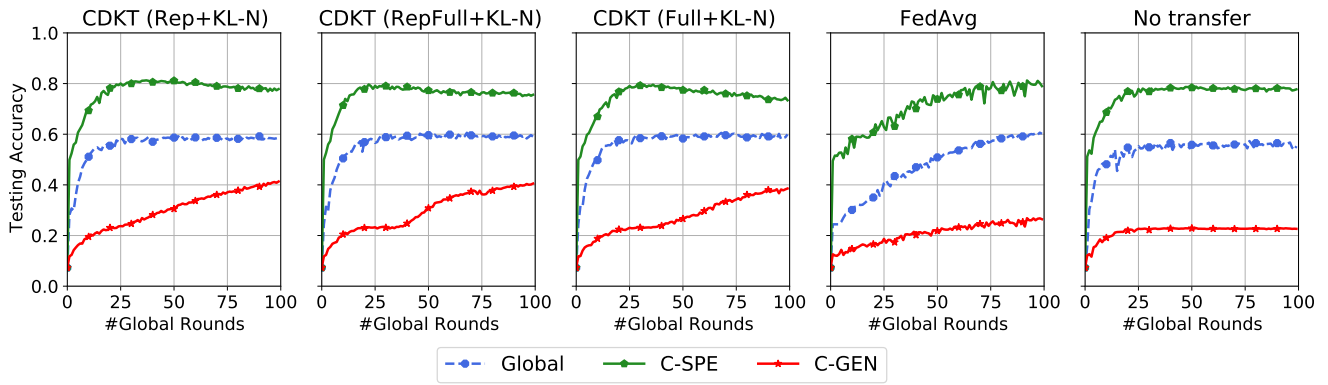


(a) Fixed Users Scenario

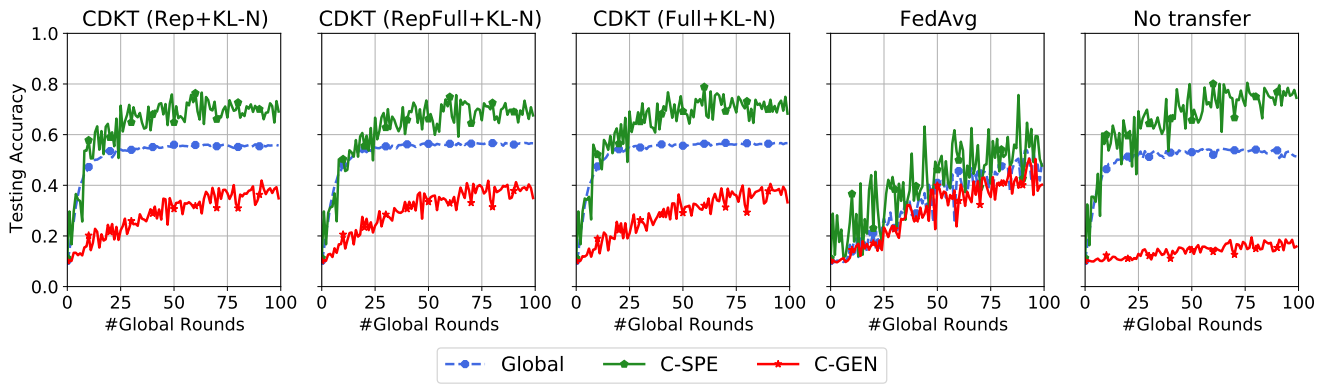


(b) Subset of Users Scenario

Figure 11: Convergence of CDKT-FL with different settings versus FedAvg with MNIST dataset



(a) Fixed Users Scenario



(b) Subset of Users Scenario

Figure 12: Comparison of CDKT-FL with different settings versus FedAvg and No Transfer with CIFAR-10 dataset

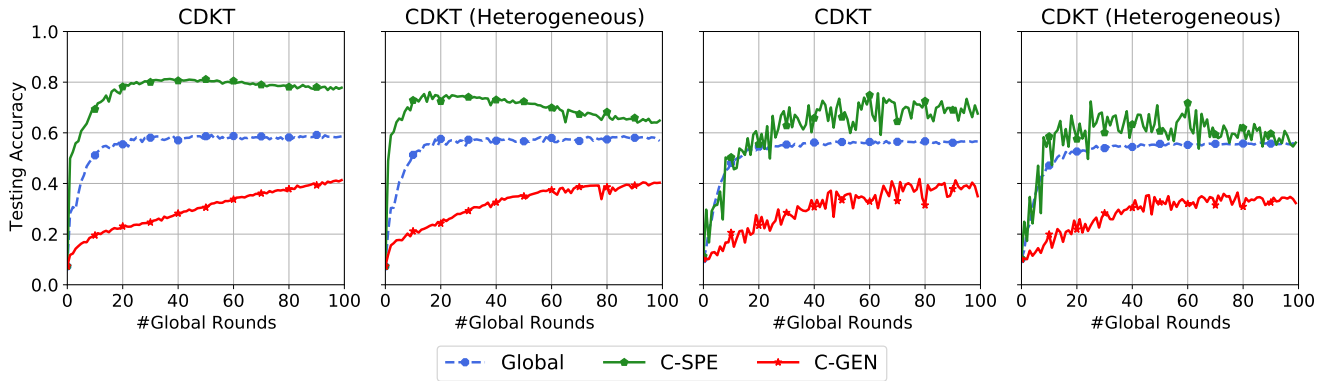
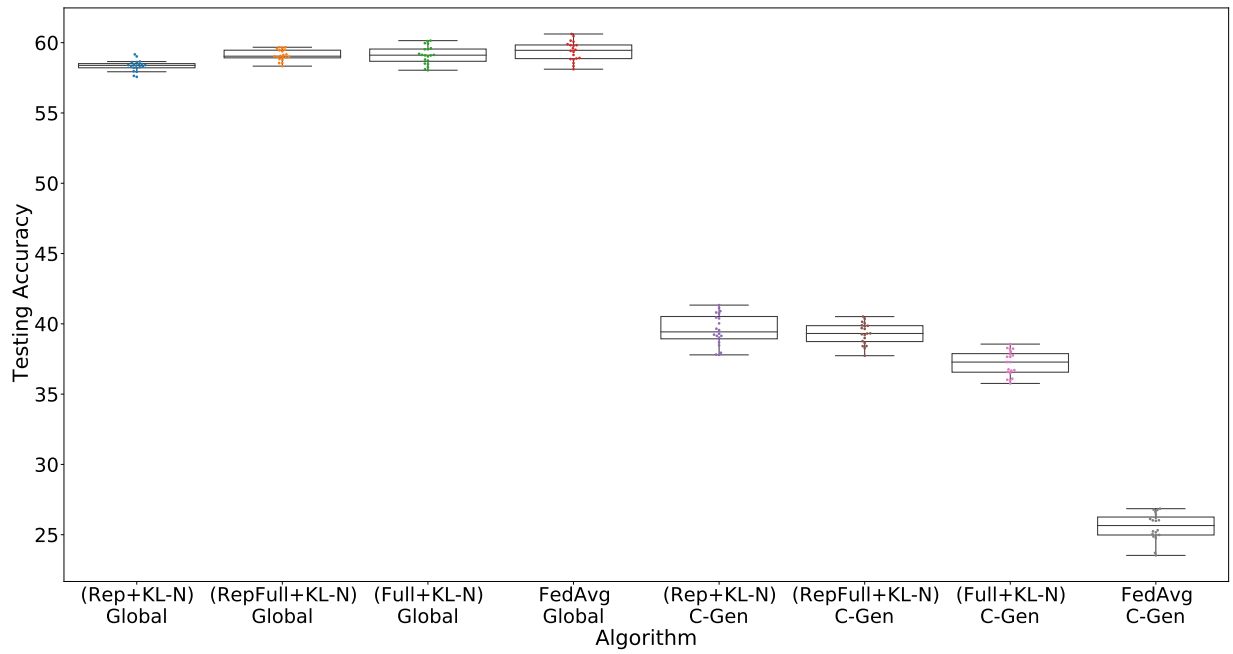
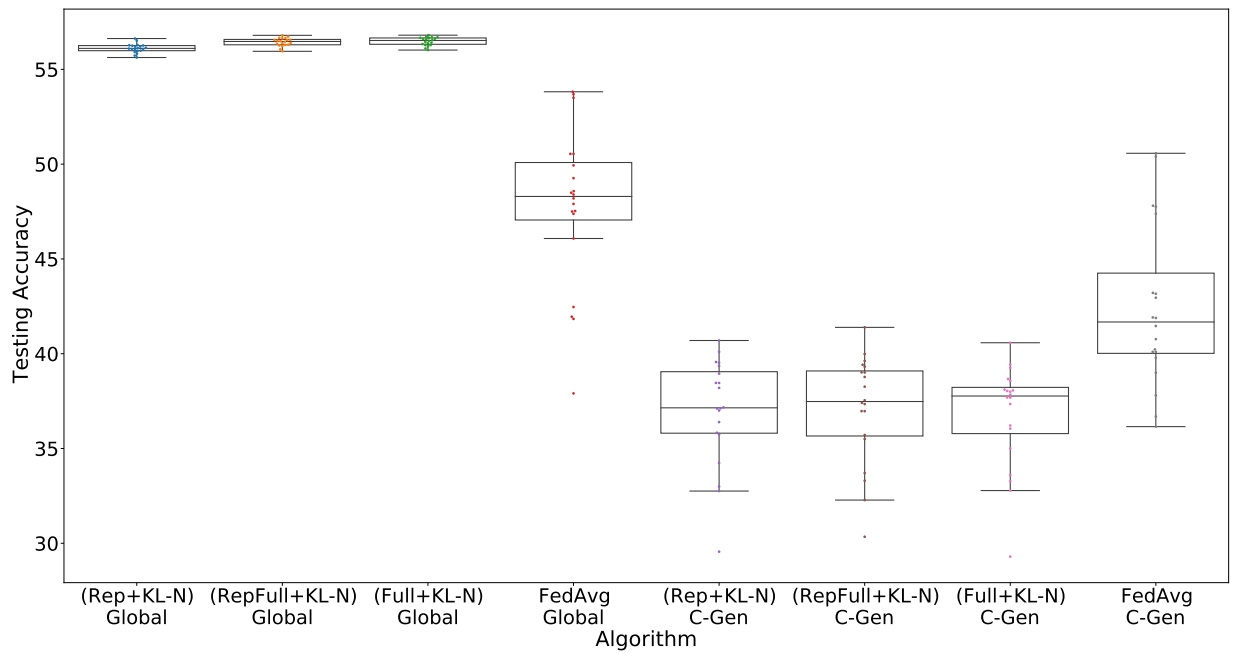


Figure 13: Comparison between Homogeneous and Heterogeneous Model with CIFAR-10 dataset

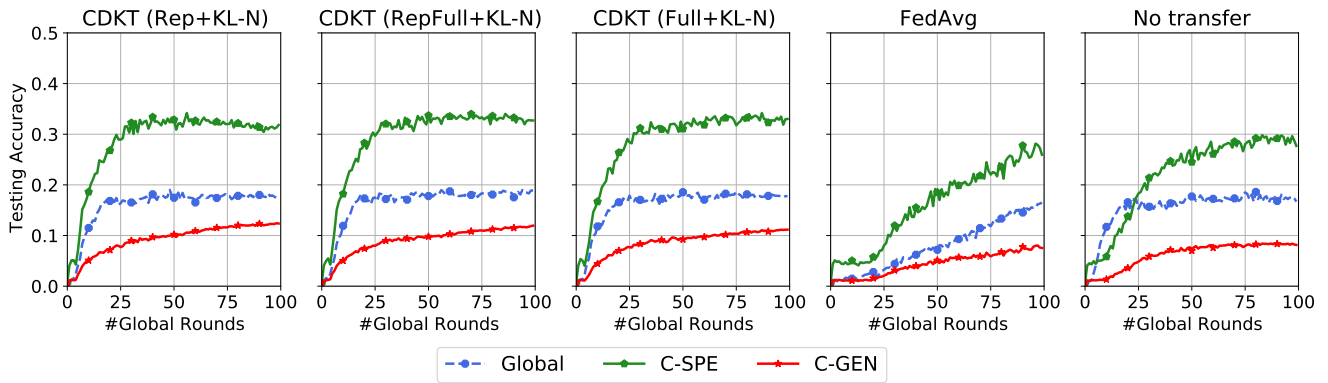


(a) Fixed Users Scenario

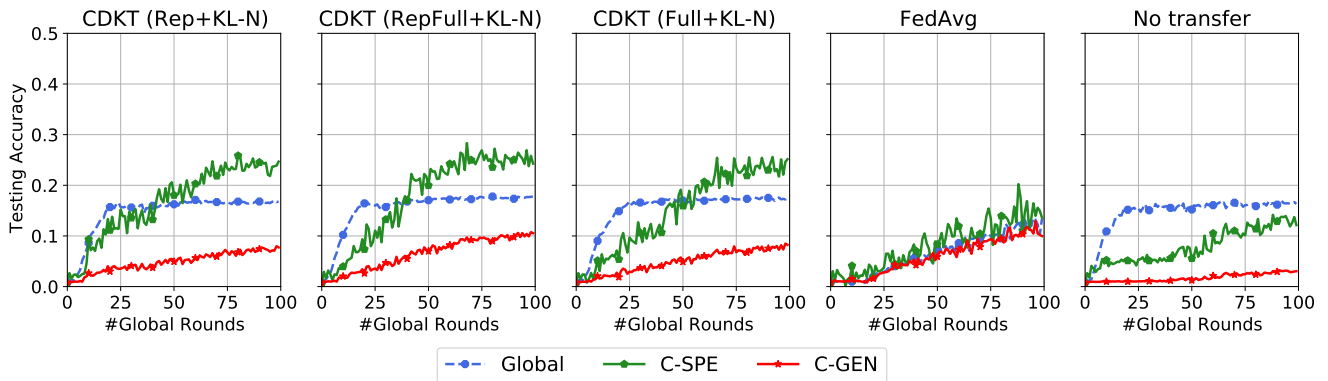


(b) Subset of Users Scenario

Figure 14: Convergence of CDKT-FL with different settings versus FedAvg with CIFAR-10 dataset



(a) Fixed Users Scenario



(b) Subset of Users Scenario

Figure 15: Comparison of CDKT-FL with different settings versus FedAvg and No Transfer with CIFAR-100 dataset

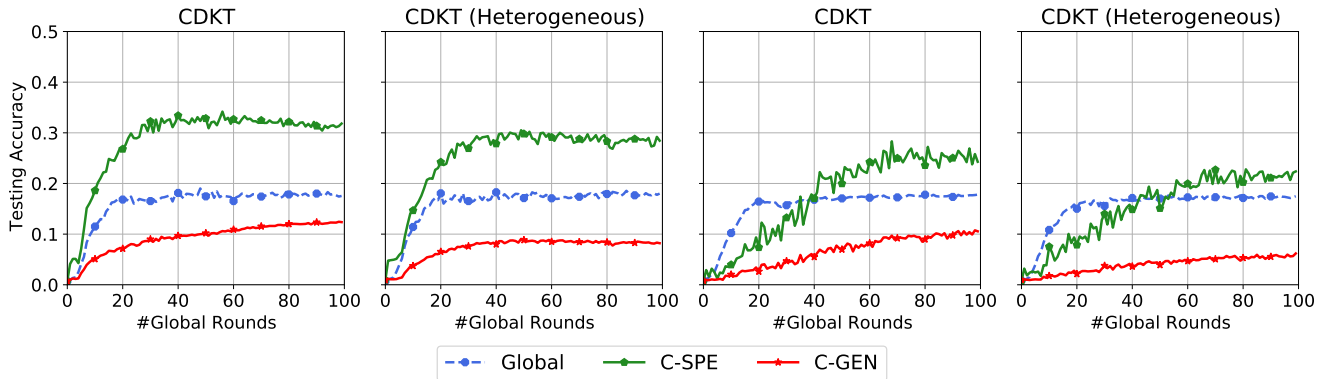
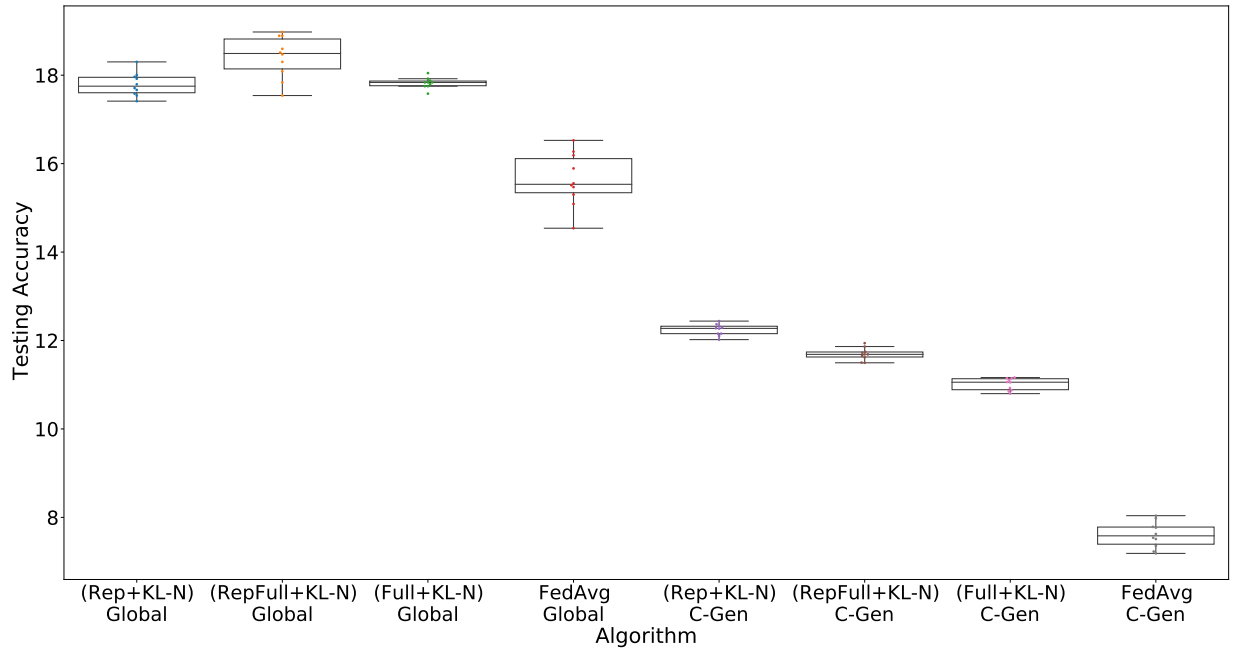
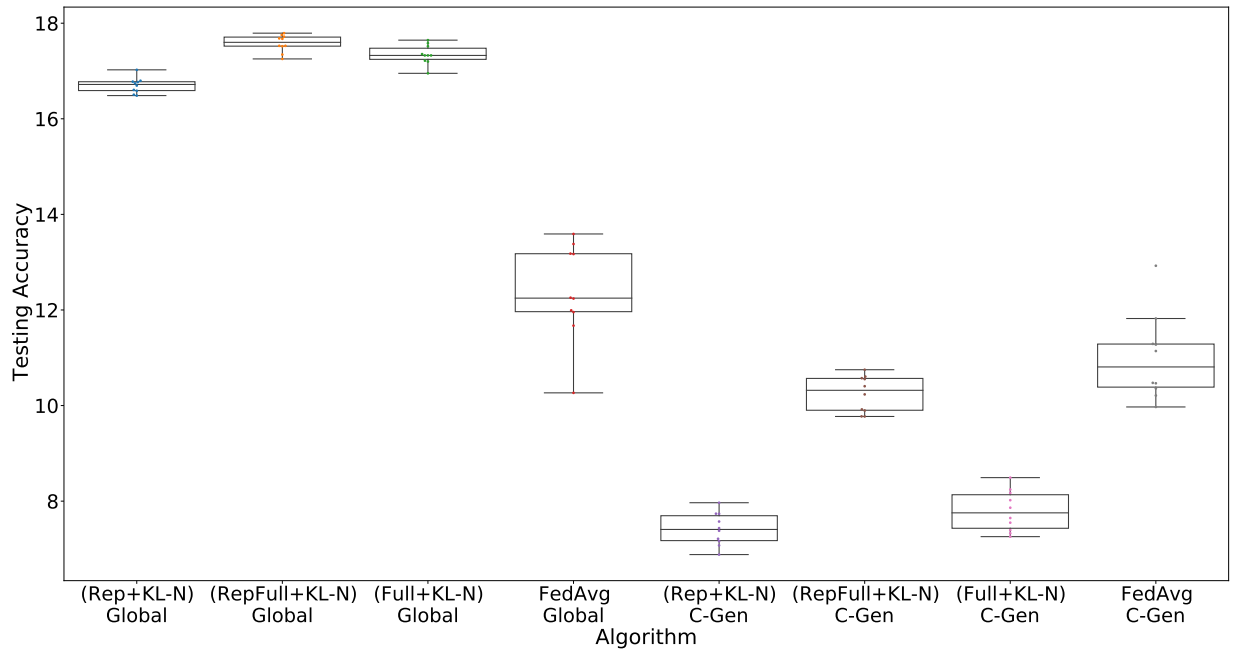


Figure 16: Comparison between Homogeneous and Heterogeneous Model with CIFAR-100 dataset



(a) Fixed Users Scenario



(b) Subset of Users Scenario

Figure 17: Convergence of CDKT-FL with different settings versus FedAvg with CIFAR-100 dataset